



## Cosmic Muon Measurement using Two NaI (TI) Radiation Detectors

Junghyun Bae\*

School of Nuclear Engineering, Purdue University, West Lafayette, IN, United States

\*Corresponding author: [bae43@purdue.edu](mailto:bae43@purdue.edu)

### Abstract

Muon is the most plentiful cosmic ray particle on Earth. At sea level, about  $10^4/\text{m}^2$  min of muons reach the ground. It is difficult to detect a cosmic muon because it has a high-penetrative feature and a short mean lifetime (2.2  $\mu\text{sec}$ ). However, we can detect it because a cosmic muon has multiple Coulomb interactions with materials due to its negative charge and it often induces Cerenkov radiation traveling within the medium. In addition, a fast-moving muon has a longer lifetime according to the Einstein's theory of special relativity. Here we show that we can observe cosmic muons indirectly in the laboratory using two radiation detectors with a coincidence logic gate. NaI scintillation crystal is used to produce photons from muon interactions and the photomultiplier tube is used to amplify signals. Recorded signals from a detector are transferred to the discriminator to separate muon signals from electronic noise and external radiation sources. Only coincident signals from two independent detectors are finally recorded as cosmic muon signals. Our experiment results are compared with a known empirical relation (cosine-squared law), which describes the correlation between cosmic muon intensity and its incident zenith angle, to verify our measurements. We expect students can learn a) energetic astroparticle, a muon, b) principles of the radiation detector, and c) Einstein's theory of special relativity.

**Keywords:** Cosmic muons, Radiation detector, Einstein's theory of special relativity.

**Copyright © 2021 The Author(s):** This is an open-access article distributed under the terms of the Creative Commons Attribution 4.0 International License (CC BY-NC 4.0) which permits unrestricted use, distribution, and reproduction in any medium for non-commercial use provided the original author and source are credited

## INTRODUCTION

Muon is one of the fundamental particles and the most common astroparticle on Earth. Understanding of astroparticle including muons is essential to learners and educators to understand modern physics. Unfortunately, astroparticles are generally impalpable, suggesting we can neither see nor feel without electronic aids. Therefore, we need an indirect measurement technique to detect cosmic muon. Here we show that a simple and economical experiment installation to provide an idea to teachers, physics educators. Students can see the practical example of time dilation by the theory of special relativity by observing plenty of cosmic muons around us. In addition, students can study properties of fundamental particles, including a muon. Lastly, students can learn the principles of the radiation detector, for example how measuring signals from radiation particles and how manipulating the original signals with the series of electronics.

In the end, throughout the muon measurement experiment, we expect that students can learn three important physics concepts:

a) Properties of energetic astroparticle, a muon.

b) Einstein's theory of special relativity.

c) Principles of the radiation detector.

For the advanced and higher education level, students also can understand:

d) Experiment instruments set up to monitor different types of incoming radiation particles.

e) An empirical relation (cosine-squared law) that describes the correlation between cosmic muon intensity and its incident zenith angle at sea level.

### Theory

#### Cosmic Muons

The standard model is analogous to the periodic table in particle physics. As the periodic table is a tabular display of the fundamental chemical elements, the standard model classifies all known elementary particles as well as known four fundamental forces. Muon is one of independent fundamental particles with the electron, tau, and their neutrinos. It is produced from Pion decay (~100%) or Kaon decay (63.5%) in the air and it has a mean lifetime of 2.2  $\mu\text{sec}$ .



**Figure-1: NaI (Tl) scintillator and PMT encapsulated the aluminium housing coupled with a preamplifier (brown cylinder).**

$$\pi^\pm = \mu^\pm + \bar{\nu}_\mu \text{ (or } \nu_\mu)$$

$$K^\pm = \mu^\pm + \bar{\nu}_\mu \text{ (or } \nu_\mu)$$

At sea level, around  $10^4/m^2$  min of cosmic muons reach to the sea level all around the world. Due to its high energetic and penetrative figure, we hardly feel their existence. For example, a 3 GeV muon in the water can penetrate greater than 10 meters. Cosmic muons are widely studied due to its promising applications. Muon tomography is initially devised by Borozdin et al [1] and geotomography [2]–[6] and spent nuclear fuel scanning [7]–[12] applications are examples.

**Einstein’s Theory of Special Relativity**

Muon is generally produced from Pion decay at an altitude of 15-20km and the published mean lifetime of a muon is 2.2  $\mu$ sec [13]. Without the theory of special relativity, cosmic muon only travels ~660 meters when a muon travels as close to the speed of light ( $v_\mu \approx c$ ). It is hardly possible that we can detect cosmic muon at sea level. However, we can measure plenty of muons in the laboratory. Because a cosmic muon travels as near the

speed of light, it must be considered as a relativistic particle. We need to introduce the Lorentz factor,

$$\gamma = \frac{1}{\sqrt{1-\beta^2}}$$

$$\beta = v/c .$$

Incoming cosmic muon travels at a speed of 0.999c in the air. Because it is a relativistic particle, we can expect the time dilation effect,

$$\Delta t' = \gamma \Delta t$$

where  $\Delta t'$  and  $\Delta t$  are the mean lifetime of a muon at moving and the rest frame, respectively. Therefore, a relativistic muon has a longer mean lifetime and moves farther. This effect allows plenty of muons to reach the ground.

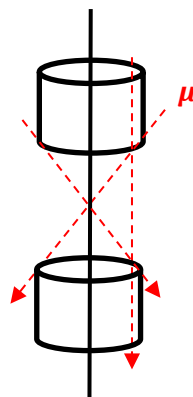


**Figure-2: Schematic diagram of measurable range and track of cosmic muon in two-scintillation detector set up.****Principles of the Radiation Detector**

In an educational purpose experiment, a scintillation detector can be used because it is inexpensive, however, it has a decent response to any type of radiations including cosmic radiations under the proper setting. Unlike the Geiger counter (well-known radiation counter), a scintillation detector can have energy spectroscopy of measuring particles using Multichannel analyzer. Unfortunately, it is challenging to measure the cosmic muon energy spectrum because a muon only loses partial energy within the detector and measurable counts are statistically too low to build a spectrum. However, we can discriminate relatively low energy particles (background radiation, noise, undesirable radiation source) by setting the high energy threshold level. Once the energetic charged particle, herein a cosmic muon, interacts with scintillation crystal, it produces photons proportional to the

**Setup**

Two scintillation detectors are placed to face each other. With this installation, we can significantly discriminate noise from muon signals. The schematic diagram of two-scintillation detectors and a few tracks of incoming muon are shown in Figure-2. The average energy of cosmic muon is about 2 GeV and incoming cosmic muon deposits partial energy by interacting with a scintillator. Interactions result in emitting scintillation photons and they produce the photoelectrons in the PMT. The deposited energy from muon to scintillators results in a signal from the preamplifier. The preamplifier output signal is transferred to the amplifier and pulse is reshaped

deposited energy. Because the number of produced photons is not enough, a silicon photomultiplier tube (SiPMT) is typically used with a scintillator in a detector. Signals are multiplied ( $\sim 10^6$ ) using PMT enough to be monitored by electronics.

**Apparatus Detectors**

Sodium Iodide (NaI) scintillation crystal and a photomultiplier tube (PMT) are encapsulated in the thin (0.020 inches) aluminum light shielding. The NaI crystal, located at the bottom of the aluminum housing, has a dimension of 5.08 cm diameter and 5.08 cm height. The photomultiplier base with the preamplifier is connected to each other as a module as shown in Figure-1. The detailed specifications of two NaI crystals, PMTs, and preamplifiers are summarized in Table-1.

electronic and thermal noise. On the other hand, the discriminator level of single channel analyzer (SCA) is fixed as maximum, 10 V to discriminate both suppressed noises and possible signals from other radiation sources. Detector systems operate independently, but they share the coincidence logic gate. Generated signals from both detector systems enter the coincidence logic gate, which only records the signal that occurred within 500 ns beyond peak detect [14]. We can free from the noises by using the coincidence logic gate.

We only measure signals simultaneously triggered at detector systems. Most of the noises can be discriminated

**Table-1: Specifications of Sodium Iodide scintillators, preamps, and PMT of two detectors [17,18]**

NaI (Tl) Scintillation detectors			Photomultiplier Base with Preamplifier	
Label	Detector I	Detector II	Model	ORTEC 276
Serial number	AA-5876-I	AA-5879-I	PMT stages	10
Manufacturer	BICRON		Conversion Gain	$10^5 - 10^6$
Model	2M2/2		Output Rise Time	< 100 nsec
Scintillator	NaI (Tl)		Output Fall Time	$\tau = 50 \mu\text{sec}$
Density	3.67 [g/cm <sup>3</sup> ]		Output Noise	< 50 $\mu\text{V}$
Crystal dimension	Diameter = 50.8 mm Thickness = 50.8 mm		Dimensions	Diameter = 56 mm Height = 102 mm
Yield	38,000 [Photons/MeV]			

to the Gaussian shape having a thinner width. Gain of the amplifier is fixed as a minimum (0.5 $\times$ 5) to suppress

since two independent detection system has little chance to measure noise coincidentally. Consequently, we selectively

detect cosmic muons. Experimental apparatus of the two-scintillation detector installation is shown in Figure-3.

**Signal output analysis**

Signal shapes from the preamplifier have an instant rising and prolonged tail. The amplitude of the signal depends on deposited energy by particles. Therefore, we can assume that two noticeable preamplifier pulses that recorded coincidentally (Figure-4), are produced by a high-energy muon. None of other radiation can produce that large pulse in our experimental environment. The signals from the amplifier are saturated (12.2 V) since the preamplifier signals are too strong, even the amplifier gain is minimum ( $\times 2.5$ ). Pulse shapes from the amplifier are shown in Figure-5 showing narrow pulse widths (3  $\mu$ sec). SCA pulses have a short pulse width (500 nsec) suggesting that it is impossible to record signals from noises unless it is generated from a single high-energy and fast particle.

**Results**

In this experiment, we measure cosmic muons in seven different zenith angles from 0 to 90 degrees with an interval of 15 degrees (0°, 15°, ... , 90°). The measurements have been performed for 24 hours in order to minimize the muon flux variance upon a time in a day. An example of the experiment instrument installations is shown in Figure-6. To verify our experiment results, we compared our

results with a cosine-squared law [15], which describes a relation between cosmic muon intensity and zenith angle at sea level.

$$I(\theta) = I_0 \cos^2 \theta$$

where,  $\theta$  is a zenith angle,  $I$  is a cosmic muon intensity, and  $I_0 = I(\theta = 0)$ .

For comparison, normalized muon counts with error bars are shown in Figure-7 with a cosine-squared law as a function of the zenith angle. For the error analysis, the standard error propagation equation is used:

$$E_A^2 = \left(\frac{\partial A}{\partial B}\right)^2 E_B^2 + \left(\frac{\partial A}{\partial C}\right)^2 E_C^2$$

where  $A = f(B, C)$ , and  $E_i$  represents an error of  $i$  component.

Normalized counts are well agreed with cosine-squared law mostly within an error level in low zenith angles ( $\theta \leq 45^\circ$ ). However, the relative errors with experiment results and cosine-squared law become larger in high zenith angles ( $\theta \geq 60^\circ$ ). It is a limit of the simple cosine-squared model.

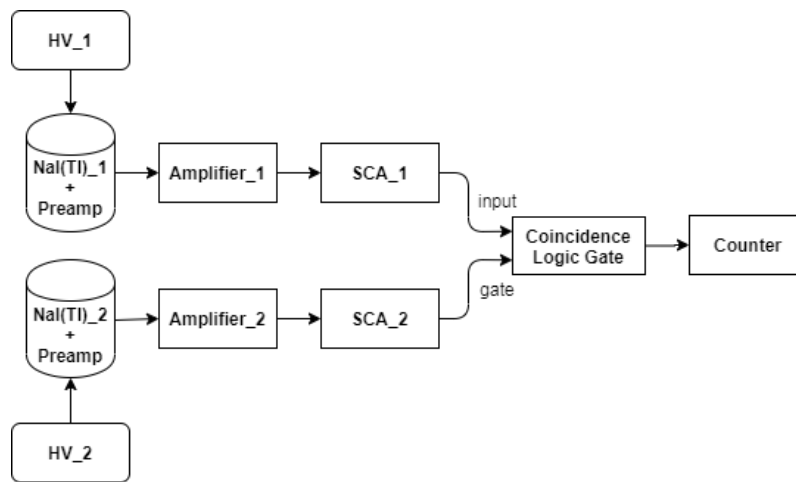


**Figure-3:** Apparatus of two-scintillation detector installation showing that two independent scintillation detector systems (scintillator, PMT, preamplifier, amplifier, and SCA) send signals to the coincidence logic gate for selective measurements.

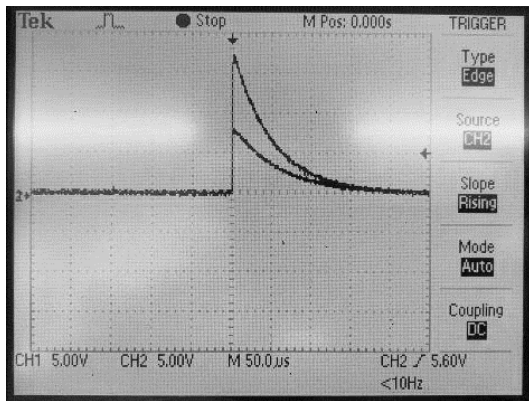


**Figure-4:** Output pulses from the preamplifier of both detectors. Pulse height is proportional to the deposited energy by incoming particles. A tall pulse represents a signal from the upper detector and a short pulse represents a signal from the lower detector.

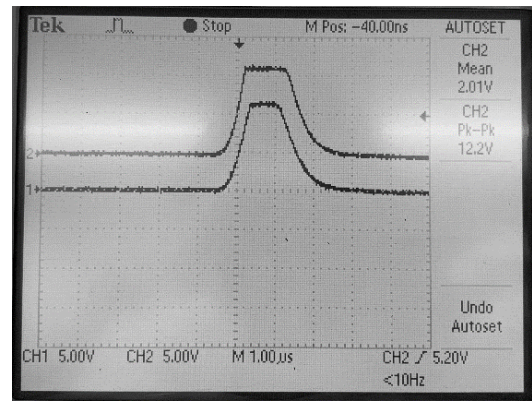


**Figure-5:** Output pulses from the amplifier of both detectors. Pulses are saturated due to the electronic limits. However, a narrow pulse width decreases system dead time. Different baselines are used for pulses from the upper detector (top) and lower detector (bottom).

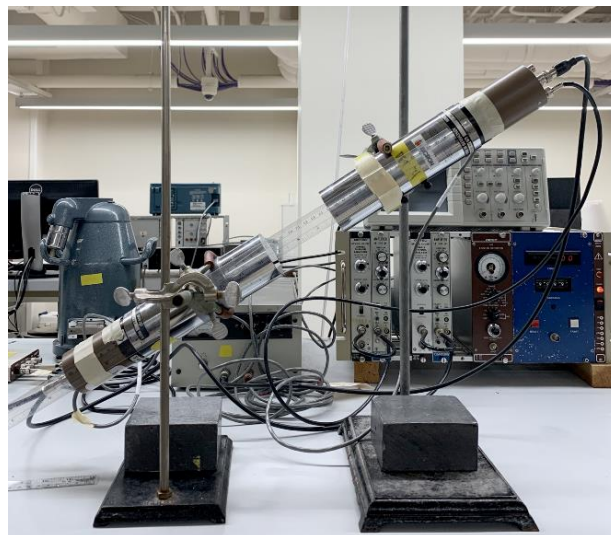


**Figure -6:** Two NaI (Tl) scintillation detectors alignment heading a zenith angle 60°.

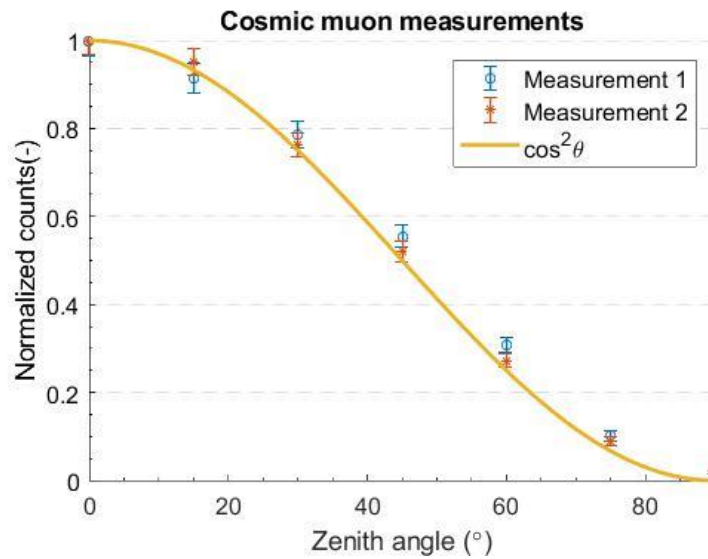


**Figure-7: Cosine-squared law and normalized cosmic muon counts. Measurements were performed twice and both measurements show good agreement with a cosine-squared model.**

For an educational purpose, enlarged relative errors at high zenith angles can be ignored, but the advanced research shows the analytical and numerical solutions for them [16].

## DISCUSSION AND CONCLUSION

In this paper, we show the methodology for measuring cosmic muons with simple and economical experimental instruments in the laboratory. As background knowledge, we discuss a) properties of a cosmic muon, b) theory of special relativity, and c) principles of radiation detectors. For the advance education, we also present the details about the detection system, apparatus in Section 3 and Section 4. We measured cosmic muon counts for 24 hours to suppress any variance during a day. The normalized experiment results are plotted in Figure-7 with errors to compare with the cosine-squared law. Elaborate manipulation of electronics including amplifier, SCA allows us to discriminate background noise and outside radiation signals from energetic muon signals. In addition, we filtered out randomly appearing high-energy signals by using a coincidence logic gate, which only records simultaneous signals coming into the gate. Consequently, we successfully measured cosmic muons and we verified that our experimental results have good agreement with a cosine-squared relation.

In the class, it is difficult to measure seven data points (each zenith angle) for 24 hours. Therefore, we suggest the proper measurement time for each measurement as about 10 minutes. According to our results, we can expect 15 counts at  $\theta=0^\circ$ , and 0.5 counts at  $\theta=90^\circ$  for 10 minutes. Count rates can be increased by placing two detectors close. This count rate is statistically enough to analysis cosmic muons in the class.

## Acknowledgements

This project is supported by School of Nuclear Engineering, Purdue University.

## REFERENCES

1. Borozdin, K. N., Hogan, G. E., Morris, C., Priedhorsky, W. C., Saunders, A., Schultz, L. J., & Teasdale, M. E. (2003). Radiographic imaging with cosmic-ray muons. *Nature*, 422(6929), 277-277.
2. Schouten, D., & Ledru, P. (2018). Muon tomography applied to a dense uranium deposit at the McArthur River Mine. *Journal of Geophysical Research: Solid Earth*, 123(10), 8637-8652.
3. Schouten, D. (2019). Muon geotomography: selected case studies. *Philosophical Transactions of the Royal Society A*, 377(2137), 20180061.
4. Morishima, K., Kuno, M., Nishio, A., Kitagawa, N., Manabe, Y., Moto, M., ... & Tayoubi, M. (2017). Discovery of a big void in Khufu's Pyramid by observation of cosmic-ray muons. *Nature*, 552(7685), 386-390.
5. Buontempo, S., D'auria, L., De Lellis, G., Festa, G., Gasparini, P., Iacobucci, G., ... & Zollo, A. (2010). Perspectives for the radiography of Mt. Vesuvius by cosmic ray muons. *Earth, planets and space*, 62(2), 131-137.
6. Del Santo, M., Catalano, O., Mineo, T., Cusumano, G., Maccarone, M. C., La Parola,

- V., ... & Zuccarello, L. (2017). A new technique for probing the internal structure of volcanoes using cosmic-ray muons. *Nuclear and particle physics proceedings*, 291, 122-125.
7. Gnanvo, K., Grasso III, L. V., Hohlmann, M., Locke, J. B., Quintero, A., & Mitra, D. (2011). Imaging of high-Z material for nuclear contraband detection with a minimal prototype of a muon tomography station based on GEM detectors. *Nuclear Instruments and Methods in Physics Research Section A: Accelerators, Spectrometers, Detectors and Associated Equipment*, 652(1), 16-20.
  8. Frazão, L., Velthuis, J. J., Maddrell-Mander, S., & Thomay, C. (2019). High-resolution imaging of nuclear waste containers with Muon Scattering Tomography. *Journal of Instrumentation*, 14(08), P08005.
  9. Poulson, D., Durham, J. M., Guardincerri, E., Morris, C. L., Bacon, J. D., Plaud-Ramos, K., . & Hecht, A. A. (2017). Cosmic ray muon computed tomography of spent nuclear fuel in dry storage casks. *Nuclear Instruments and Methods in Physics Research Section A: Accelerators, Spectrometers, Detectors and Associated Equipment*, 842, 48-53.
  10. Clarkson, A., Hamilton, D. J., Hoek, M., Ireland, D. G., Johnstone, J. R., Kaiser, R., ... & Zimmerman, C. (2014). GEANT4 simulation of a scintillating-fibre tracker for the cosmic-ray muon tomography of legacy nuclear waste containers. *Nuclear Instruments and Methods in Physics Research Section A: Accelerators, Spectrometers, Detectors and Associated Equipment*, 746, 64-73.
  11. Riggi, S., Antonuccio-Delogo, V., Bandieramonte, M., Becciani, U., Costa, A., La Rocca, P., ... & Vitello, F. (2013). Muon tomography imaging algorithms for nuclear threat detection inside large volume containers with the Muon Portal detector. *Nuclear Instruments and Methods in Physics Research Section A: Accelerators, Spectrometers, Detectors and Associated Equipment*, 728, 59-68.
  12. Jonkmans, G., Anghel, V. N. P., Jewett, C., & Thompson, M. (2013). Nuclear waste imaging and spent fuel verification by muon tomography. *Annals of Nuclear Energy*, 53, 267-273.
  13. Baudis, L., Zyla, P. A., Barnett, R. M., Beringer, J., Dahl, O., Dwyer, D. A., ... & Yao, W. M. (2020). Review of Particle Physics. *Progress of Theoretical and Experimental Physics*, 2020(8), 083C01.
  14. Davies, H. S., Rosas-Moreno, J., Cox, F., Lythgoe, P., Bewsher, A., Livens, F. R., ... & Pittman, J. K. (2018). Multiple environmental factors influence <sup>238</sup>U, <sup>232</sup>Th and <sup>226</sup>Ra bioaccumulation in arbuscular mycorrhizal-associated plants. *Science of the Total Environment*, 640, 921-934.
  15. Grieder, P. K. (Ed.). (2001). *Cosmic rays at Earth*. Elsevier.
  16. Bae, J., Chatzidakis, S., & Bean, R. (2021). Effective Solid Angle Model and Monte Carlo Method: Improved Estimations to Measure Cosmic Muon Intensity at Sea Level in All Zenith Angles. arXiv preprint arXiv:2102.01204.
  17. ORTEC 2005 Model 276 Photomultiplier Base Operating and Service Manual Advanced Measurement Technology
  18. Peralta, L. (2018). Temperature dependence of plastic scintillators. *Nuclear Instruments and Methods in Physics Research Section A: Accelerators, Spectrometers, Detectors and Associated Equipment*, 883, 20-23.